

Direct Functionalization of the Hydroxyl Group of the 6-Mercapto-1-hexanol (MCH) Ligand Attached to Gold Nanoclusters

Hua Tan, Tong Zhan, and Wai Yip Fan*

Department of Chemistry, National University of Singapore, 3 Science Drive 3, Singapore 117543, Singapore

Received: August 31, 2006

Au-MCH nanoclusters of (1.5 ± 0.3) nm diameter (MCH = 6-mercapto-1-hexanol, $\text{HS}-(\text{CH}_2)_6\text{-OH}$) have been prepared and characterized by Transmission Electron Microscopy (TEM), UV–visible, Nuclear Magnetic Resonance (NMR), Fourier Transform Infrared (FTIR) absorption spectroscopies, X-ray Powder Diffraction (XRD), and Thermogravimetric Analysis (TGA). While in nanocluster form dispersed in solution, the OH terminal group of the MCH ligand has been directly functionalized through small organic molecule reactions in near-quantitative yield ($>90\%$) to generate ester, carbamate, carboxylic acid, nitrite, and aldehyde groups, as recorded by FTIR spectroscopy. The size of the final gold nanocluster derivative is preserved for all the reactions studied here.

Introduction

Functionalized monolayer-protected gold nanoclusters have been intensively studied due to their potential uses in nano-electronic devices,¹ medical diagnostics,² drug delivery,³ and catalysis.⁴ Efforts aimed toward controlling their chemical and physical properties have focused on adjusting the gold nanocluster size. An approach described by the Murray group⁵ is to use place-exchange reactions which rely on the replacement of surface ligands by ω -functionalized alkanethiols to produce chemically useful nanoparticles. Direct functionalization of ligands adsorbed on gold and silver thin films with various organic reactants has also been achieved^{6,7} but similar work on gold nanoclusters dispersed in solution has received little attention. Although it is possible to first synthesize ligands with bifunctional groups, MCH ($\text{HS}-(\text{CH}_2)_6\text{-OH}$), for example, and then attach them onto gold nanoclusters, the SH functional group required for gold attachment often takes part in the reaction and thus loses its adsorption properties. Direct functionalization of the surfactants on the nanoclusters becomes desirable since the SH group can first be inactivated once attached to the gold nanocluster, leaving only the other group (OH) to undergo subsequent reactions. However, it is unclear whether the gold particle size will be affected or complete detachment of the surfactants will occur or even different reaction pathways will be observed. Only recently Fleming et al. showed that a bromine-terminated surfactant on Au nanoclusters could be directly reacted with an azide group to yield triazoles.⁸ As the OH group in a typical organic molecule has been used for derivatization to yield many important functionalities such as bromide, aldehyde, acid, and ester, the Au-MCH nanocluster has been chosen in this work to highlight the versatility of using its terminal OH group in direct functionalization without perturbing the size of the gold nanocluster. Near-quantitative yields of the nanoclusters were also obtained for all the reactions chosen to react with OH under room temperature conditions.

Experimental Section

The general functionalization strategy is shown in Scheme 1 and a more detail description of the procedures is given below.

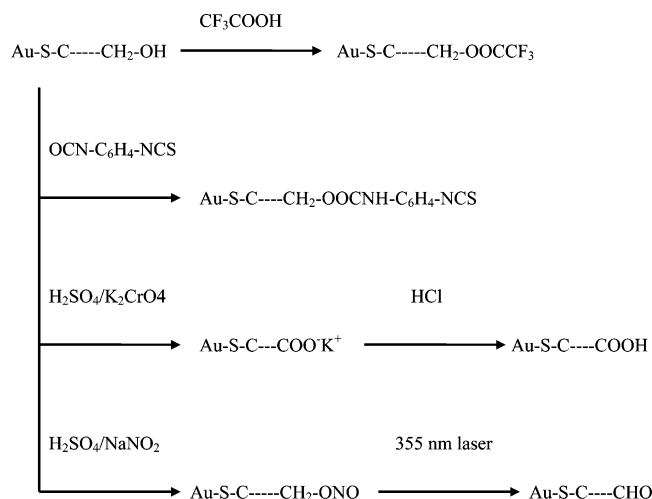
Au-MCH Nanoparticle Synthesis. Au-MCH nanoparticles were synthesized according to a modified literature procedure.⁹ Briefly, tetrachloroaurate trihydrate, $\text{HAuCl}_4 \cdot 3\text{H}_2\text{O}$ (0.1 g, 0.254 mmol), and excess tetraoctylammonium bromide, $(\text{C}_8\text{H}_{17})_4\text{N}^+\text{Br}^-$ (0.56 g, 1.03 mmol), were dissolved in a water/toluene mixture (30 mL/50 mL). When the organic phase turned golden, MCH (0.136 g, 1.01 mmol) was added and the solution was stirred vigorously for 10 min until the organic phase became white and cloudy. Aqueous sodium borohydride (96 mg, 2.54 mmol, dissolved in 5 mL of water immediately prior to use) was rapidly added and the organic phase immediately turned dark brownish. Dark precipitate appeared in toluene. This solution was stirred for another half an hour before the resulting solid was washed with a series of solvents (toluene, acetone, hexane, acetone/water (5:1)) to remove the phase transfer catalyst, byproducts, and unreacted starting materials. After purification, the yield is 34.7% (17 mg of purified Au-MCH nanoparticles).

Functionalization of Au-MCH with Organic Reagents. A THF solution containing 50 mg of Au MCH and 1 mmol of CF_3COOH was stirred for 48 h at room temperature, with the resulting product readily precipitated upon addition of excess water to the mixture. The precipitate was isolated by centrifugation at 2000 rpm, washed with water to remove CF_3COOH , and stored in a vacuum desiccator.

For the reaction of Au-MCH with $\text{NCS}-\text{C}_6\text{H}_4\text{-NCO}$, a THF solution containing 50 mg of Au MCH and 2.33 mmol of $\text{NCS}-\text{C}_6\text{H}_4\text{-NCO}$ was stirred for 48 to 72 h at room temperature with the resulting product precipitated upon addition of excess toluene. The product was isolated by centrifugation, washed with toluene to remove unreacted $\text{NCS}-\text{Ph}-\text{NCO}$, and stored in a vacuum desiccator.

For the oxidation of Au-MCH, an acetone/water (1:1) solution containing 50 mg of Au MPCs, 3.35 mmol of H_2SO_4 , and 3.41 mmol of K_2CrO_4 was stirred for 48 h at room temperature with the product precipitated upon addition of excess acetone, isolated by centrifugation, and washed further with acetone and acetone/

* Address correspondence to this author. E-mail: chmfanwy@nus.edu.sg.
Fax: 65-67791691.

SCHEME 1: Reaction Schemes for Functionalizing Au-MCH Nanoparticles

water (5:1) mixture. Further derivatization was carried out by adding 0.2 M HCl into water containing the dispersed nanoparticles. Purification by dialysis against pure water was performed for 8 h before the resulting solid Au nanoparticles were collected and stored in a vacuum desiccator.

For the reaction of Au-MCH with NaNO_2 , 50 mg of Au MPCs, 2.15 mmol of H_2SO_4 , and 3.13 mmol of NaNO_2 were dissolved in an acetone/water (1:1) mixture and stirred for 48 h at room temperature. The precipitate obtained upon addition of excess water was isolated by centrifugation and washed with water and acetone/water (1:4). The solid was redispersed in acetone and irradiated with a 355 nm Nd:YAG pulse laser (Continuum Surelite III-10, 8–10 ns pulse) at 15 mJ/pulse for 3 h. The resulting product was readily precipitated upon addition of excess water to the reaction mixture and isolated by centrifugation and stored in a vacuum desiccator.

For ^1H NMR studies, the various nanoparticles have been reacted with iodine in order to detach the ligands from gold by cleaving the gold–sulfur interaction.⁸ Briefly, 6 mg of I_2 was added into 50 mg of Au nanoparticles dissolved in ethanol solution, and after 3 to 4 h of stirring, the black precipitate was removed by centrifugation. The solution was evaporated to dryness, and the remaining product (liquid or solid) was dissolved in CDCl_3 for NMR (300 MHz) characterization.

Results and Discussion

The Au-MCH nanoclusters were first characterized by a variety of techniques before embarking on the functionalization work. A TEM (JEOL 3010, 300 keV) image in Figure 1a shows narrowly dispersed nanoparticles of (1.5 ± 0.3) nm diameter. Its UV–visible absorption spectrum in Figure 1b exhibits a weak surface plasmon resonance band centered at 520 nm, which is indicative of the formation of gold nanoclusters of diameters less than 2 nm.¹⁰ Consistent with the TEM measurement, the powder XRD pattern (Siemens D5005, $\text{Cu K}\alpha$ $\lambda = 0.15418$ nm) of the Au-MCH solid sample in Figure 2a shows the average nanocluster size calculated with use of Scherrer's formula to be 1.6 nm, based on the width of the (111) peak. A TGA graph in Figure 2b indicates that 81% of the same sample is gold by mass.

The percentage weight loss is explained by estimating the ligand mass fraction in the sample. If a close-packed surfactant monolayer on the surface of a nanoparticle of diameter D is assumed, the total weight W of the nanoparticle plus the

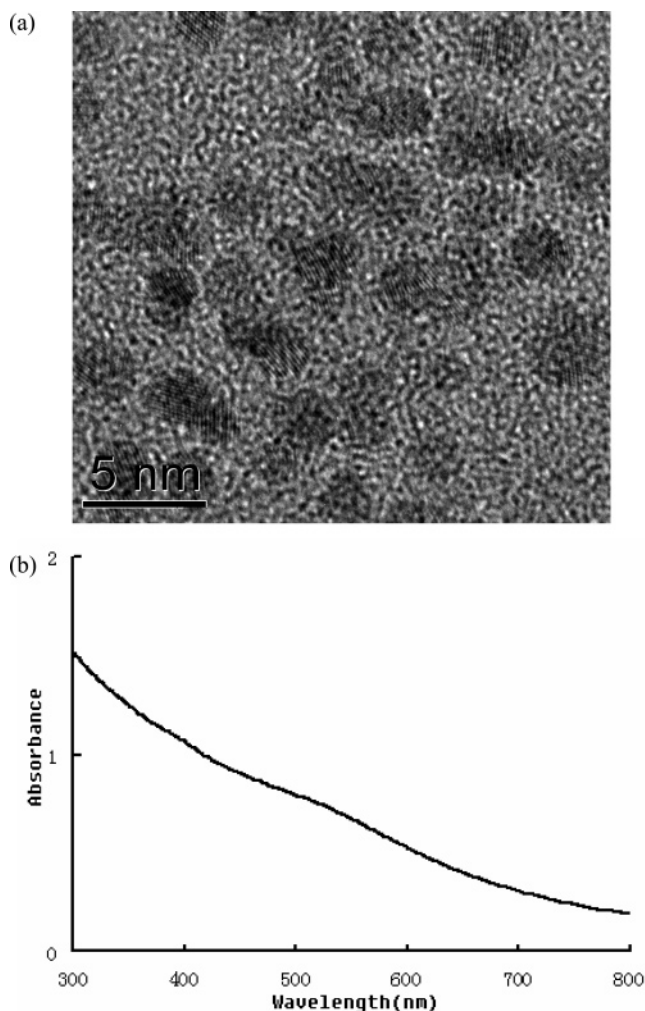


Figure 1. (a) TEM image showing a closeup image (with lattice spacing) of Au-MCH nanoparticles of 1.5 ± 0.3 nm diameter. (b) UV–visible absorption spectrum of the Au-MCH nanoparticles in solution.

monolayer is $(1/6)\pi D^3\rho + (\pi D^2/a)(M/N_0)$, where D = mean diameter (1.6 nm), ρ = the density of the particle (19.3 g/cm^3), a = the head area per surfactant molecule (21.4 \AA^2), M = the molecular weight of the surfactant (134 amu), and N_0 = Avogadro's number.¹¹ Assuming the TGA heating causes weight loss of only the surfactants, the percentage weight loss from a particle is $100\% \times (\pi D^2/a)(M/N_0)/W$. From this equation, the calculated loss is about 17%, in good agreement with the TGA value of 19%. The small discrepancy here may lie with the use of the mean size rather than considering the actual size distribution of the Au-MCH nanoclusters.

Solid-state FTIR spectroscopy has been utilized for the characterization of the various new functional groups attached to the Au nanoclusters. The functional groups were chosen such that they possess intense IR signals for easier detection, such as a carbonyl (CO) stretch. The FTIR spectrum of solid Au-MCH in Figure 3a shows much similarity to that obtained for the pure MCH molecule except that the SH vibrational band at 2550 cm^{-1} has disappeared as it has been replaced by an Au–S bond. This is typical of many alkanethiols adsorbed on gold surfaces as observed by using the Surface-Enhanced Raman Scattering (SERS) technique.^{12,13} The spectrum contains three characteristic peaks, namely two alkyl stretching vibrations between 2800 and 3000 cm^{-1} and the C–O–H bending vibration around 1620 cm^{-1} . Although the O–H stretching vibration around 3373 cm^{-1} could also be seen, this region

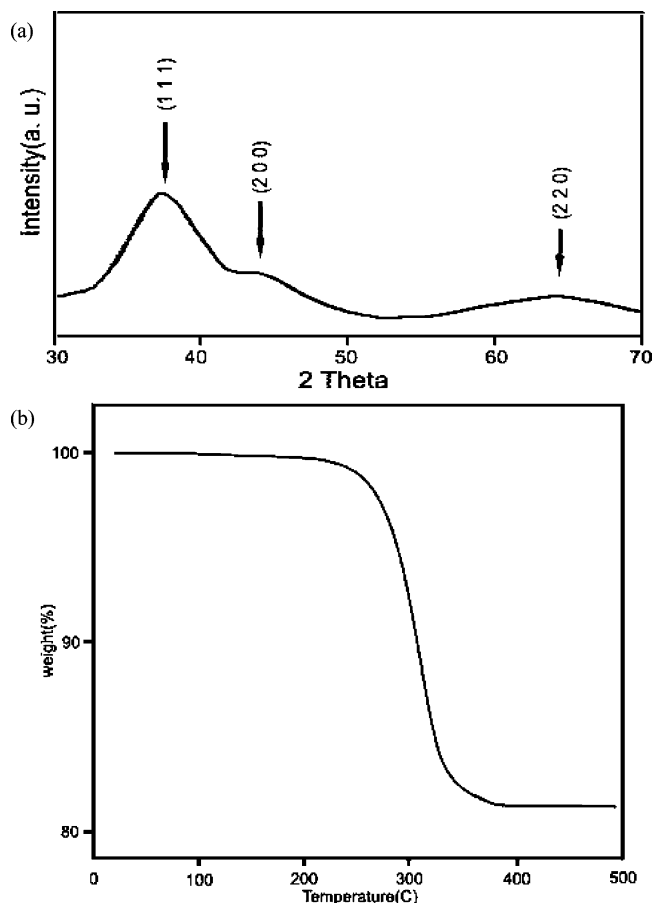


Figure 2. (a) XRD spectrum and (b) TGA profile of Au-MCH nanoclusters.

(3300–3500 cm^{-1}) contains significant contributions from the O–H stretching vibrations of water. Because of the difficulty of drying the samples completely, this band could not be used for diagnostic purposes. Similar to the FTIR studies of monolayer-protected Au clusters, the presence of the symmetric and antisymmetric C–H stretching modes indicates that the alkyl chains of Au-MCH are also adopting the well-ordered trans orientation.¹⁴ In comparison, the FTIR spectrum of the Au nanoparticles after esterification with CF_3COOH (Figure 3b) contains a new intense vibrational band at 1787 cm^{-1} . This is assigned to the CO stretch of the $-\text{COO}$ ester group. The alkyl stretching vibrations have shifted 1 or 2 cm^{-1} compared with those for the Au-MCH nanoclusters suggesting that the esterification did not perturb the structure of the monolayer on the nanoparticle surface. As expected the C–O–H bending vibration disappears as it has been replaced by a C–O–COOCF₃ moiety. The fingerprint regions for Au-MCH and the Au-ester nanoclusters are found to be very different, with no significant trace of Au-MCH signals in the latter spectrum, which demonstrates that Au-MCH has undergone near-complete functionalization with yield at least 90%. We found no difference in its UV–visible spectra of the Au nanoclusters before and after esterification. The TEM images also showed similar sizes for the newly functionalized Au-ester nanoclusters. In fact, for all the reactions studied here, the size of the Au nanoclusters is preserved, as monitored by UV–visible spectroscopy.

The reaction between Au-MCH nanoclusters and $\text{NCO-C}_6\text{H}_4\text{-NCS}$ also proceeds with yields in excess of 90%. Since the OH group preferentially reacts with NCO, this leaves behind the unreacted NCS group as the terminal group. Compounds of such structure have been found to display anticancer properties similar

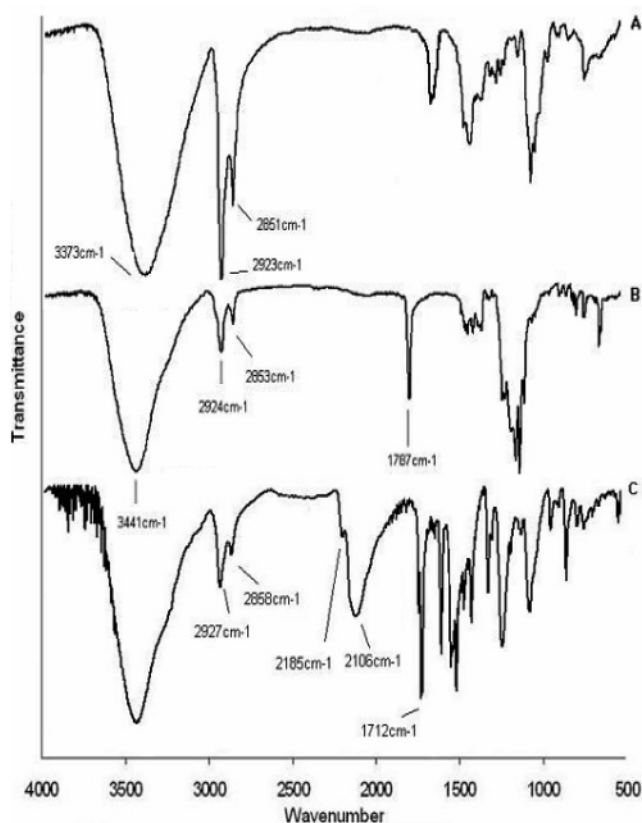


Figure 3. Solid-state FTIR spectra of (a) Au-MCH nanoclusters and Au nanoclusters after derivatization with (b) CF_3COOH and (c) $\text{SCN-C}_6\text{H}_4\text{-NCO}$.

to those of sulforaphane, $\text{CH}_3\text{S(=O)(CH}_2)_4\text{NCS}$ in broccoli.^{15,16} An Au nanoparticle containing an NCS group may thus have potential uses in the diagnostic of cancer cells. The FTIR spectrum of pure $\text{NCO-C}_6\text{H}_4\text{-NCS}$ solid has three characteristic peaks, namely the N=C=O stretch at 2272 cm^{-1} , the CO stretch at 1643 cm^{-1} , and a broad N=C=S stretch around 2143 cm^{-1} . From Figure 3c, the two peaks (2272 and 1643 cm^{-1}) belonging to NCO have disappeared due to the addition reaction between NCO and OH to form a carbamate group¹⁷ while the peak belonging to NCS shows only a small frequency shift.

The OH group can be converted into a nitrite (ONO) upon reaction with NaNO_2 in acidic conditions. Two peaks assigned to the trans and cis vibrations of ONO were observed at 1600 and 1536 cm^{-1} , respectively (Figure 4a).¹⁸ When the nitrite group is further subjected to 355 nm UV photolysis, O–NO bond cleavage occurs producing an alkoxy intermediate that undergoes further decomposition to an aldehyde (CHO) group.¹⁸ The FTIR spectrum of the final product does not show the two ONO signals anymore but a new peak that appears at 1710 cm^{-1} could easily be assigned to the CO stretching vibration of the CHO group (Figure 4b).

The conversion of OH in Au-MCH nanoclusters into the COOH group by a strong oxidant, K_2CrO_4 , has also been attempted. After reaction, the nanocluster is found to possess the COO^-K^+ group as indicated by the low-frequency CO vibration at 1600 cm^{-1} (Figure 4c). Upon dialysis in acidic conditions against pure water, the K^+ ions could be washed away and replaced by H^+ ions. A subsequent FTIR spectrum (Figure 4d) showed a shift to higher wavenumber at 1700 cm^{-1} , indicative of the conversion from a COO^-K^+ to a COOH group.

Proton NMR spectroscopy has also been used to characterize the ligands on the nanoparticles. Since NMR spectra of gold

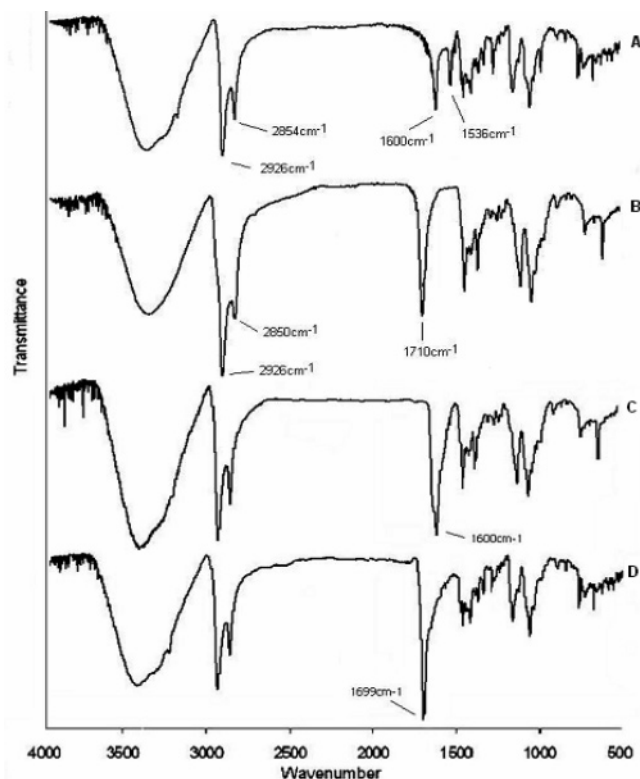


Figure 4. Solid-state FTIR spectra of Au nanoclusters after derivatization with (a) NaNO_2 , (b) subsequent 355 nm photolysis of the nitrite sample yielding an aldehyde, (c) $\text{K}_2\text{CrO}_4/\text{acid}$, and (d) dialysis with HCl of the carboxylate sample.

nanoparticles tend to be broad, we have adopted a previously reported method to prepare disulfide derivatives of the ligands by using iodine to cleave the gold–sulfur interaction.⁸ These disulfides are easily dissolved in CDCl_3 to yield typical organic NMR spectra. We have focused on obtaining spectra for two out of the four reactions investigated here, namely the nitration of Au-MCH and the reaction with the NCO- group. For the spectrum of the disulfide derivative of Au-MCH (please refer to spectra in the Supporting Information section), three main features were observed: the triplet at 3.70 ppm belongs to the terminal $-\text{CH}_2\text{-O}$ group, another triplet centered at 2.74 ppm has been assigned to the $-\text{CH}_2\text{-S}$ group, and the cluster of lines from 1.2 to 1.8 ppm is due to the protons of the $-(\text{CH}_2)_4$ chain.

The NMR spectrum for the disulfide derivative of the $-\text{ONO}$ ligand shows a large shift from 3.71 to 4.73 ppm when the $-\text{CH}_2\text{-OH}$ group was nitrated to $-\text{CH}_2\text{-ONO}$. No trace of the disulfide derivative of MCH was seen, indicating that the percentage conversion to nitrite is very high indeed, similar to the FTIR data. The NMR spectrum for the aldehyde derivative is also displayed and this time, the distinctive CHO aldehyde signal at 9.69 ppm is clearly seen. Again, the conversion from nitrite to aldehyde also appears to be complete since no trace of the 4.73 ppm signals due to the $-\text{CH}_2\text{-ONO}$ group was seen. The new group of lines shifted to 2.38 ppm is due to the methylene group next to the aldehyde, i.e., $-\text{CH}_2\text{-CHO}$ groups. The NMR spectrum of the disulfide derivatives of the $-\text{NCS}$ ligand contains the expected peaks from the aromatic ring at

7.16 (2H) and 6.96 ppm (2H) as well as the $-\text{CH}_2\text{-NCO-}$ peaks at 4.05 ppm and the $-\text{CH}_2\text{-S}$ peaks at 2.69 ppm. Again, no trace of the MCH precursor ligand was detected. Both FTIR and NMR results indicate a high yield synthesis of functionalized MCH ligands on gold.

We have shown from these four reactions that the OH group can be converted easily into other useful functional groups while preserving the gold nanocluster size and the structure of surface monolayers. Reactivity studies with the Au-MCH nanocluster itself may also be possible where one can envision the OH group reacting specifically with some species within a chemical or biological system of interest. Currently we are exploring the possibility of extending the Au nanocluster functionalization to biomolecules as well as phosphine derivatives bound to catalytically active organometallic species.

Acknowledgment. The project was supported by the Agency of Science, Technology and Research (ASTAR) under Grant No.143-000-198-305. H.T. and T.Z. thank the National University of Singapore for research scholarships.

Supporting Information Available: Proton NMR spectra for the disulfide derivative of MCH and the disulfide derivative of MCH containing the ONO group, the CHO group, and the NCS group. This material is available free of charge via the Internet at <http://pubs.acs.org>.

References and Notes

- Andres, R. P.; Bein, T.; Dorogi, M.; Feng, S.; Henderson, J. I.; Kubiak, C. P.; Mahoney, W.; Osifchin, R. G.; Reifemberger, R. *Science* **1996**, 272, 1323.
- Haes, A. J.; Hall, W. P.; Chang, L.; Klein, W. L.; Van Duyne, R. P. *Nano Lett.* **2004**, 4, 1029.
- Gupta, A. K.; Gupta, M. *Biomaterials* **2005**, 26, 3995.
- Roucoux, A.; Schulz, J.; Patin, H. *Chem. Rev.* **2002**, 102, 3757.
- Hostetler, M. J.; Green, S. J.; Stokes, J. J.; Murray, R. W. *J. Am. Chem. Soc.* **1996**, 118, 4212.
- Hutt, D. A.; Leggett, G. J. *Langmuir* **1997**, 13, 2740.
- Chechik, V.; Crooks, R. M.; Stirling, C. J. M. *Adv. Mater.* **2000**, 12, 1161.
- Fleming, D. A.; Thode, C. J.; Williams, M. E. *Chem. Mater.* **2006**, 18, 2327.
- Brust, M.; Walker, M.; Bethell, D.; Schiffrin, D. J.; Whyman, R. *J. Chem. Soc., Chem. Commun.* **1994**, 801.
- Alvarez, M. M.; Khoury, J. T.; Schaaff, T. G.; Shafigullin, M. N.; Vezmar, I.; Whetten, R. L. *J. Phys. Chem. B* **1997**, 101, 3706.
- Badia, A.; Cuccia, L.; Demers, L.; Morin, F.; Lennox, R. B. *J. Am. Chem. Soc.* **1997**, 119, 2682. Notes: The mass of a spherical Au nanoparticle is $V\rho = (1/6)\pi D^3\rho$; the surface area of the nanoparticle is πD^2 , and since the headgroup area of MCH is $a = 21.4 \text{ \AA}^2$, the mass of MCH molecules on the surface of Au nanoparticle is $(\pi D^2/a)(M/N_0)$.
- Szafranski, C. A.; Tanner, W.; Laibinis, P. E.; Garrell, R. L. *Langmuir* **1998**, 14, 3570.
- Clark, B. K.; Gregory, B. W.; Avila, A.; Cotton, T. M.; Standard, J. M. *J. Phys. Chem. B* **1999**, 103, 8201.
- Hostetler, M. J.; Stokes, J. J.; Murray, R. W. *Langmuir* **1996**, 12, 3604.
- Zhang, Y.; Kensler, T. W.; Cho, C. G.; Posner, G. H.; Talalay, P. *PNAS* **1994**, 91, 3147.
- Gerhauser, C.; You, M.; Liu, J.; Moriarty, R. M.; Hawthorne, M.; Mehta, R. G.; Moon, R. C.; Pezzuto, J. M. *Cancer Res.* **1997**, 57, 272.
- Hassner, A.; Lorber, M. E.; Heathcock, C. H. *J. Org. Chem.* **1967**, 32, 540.
- Li, S. P.; Chwee, T. S.; Fan, W. Y. *Chem. Phys.* **2006**, 320, 259.